Frontiers in Bioscience Landmark

Front. Biosci. (Landmark Ed) **2022**; 27(9): 278
https://doi.org/10.31083/j.fbl2709278

Original Research

The Effects of Tangning Ziyabitusi on Gut Microbiota and T lymphocyte Subsets in Impaired Glucose Regulation Rats

Bingyao Zhao[1,†], Rebiya Nuli[2,†], Yi Jiao[1], Bing Zhang[2], Ling Wang[2], Yaqun Guan[1,*]

[1]Department of Biochemistry and Molecular Biology, School of Basic Medical Sciences, Xinjiang Medical University, 830017 Urumqi, Xinjiang, China
[2]Department of Human Parasitology, School of Basic Medical Sciences, Xinjiang Medical University, 830017 Urumqi, Xinjiang, China
*Correspondence: yaqunguan557@xjmu.edu.cn (Yaqun Guan)
[†]These authors contributed equally.

Academic Editor: Rosa Alduina
Submitted: 28 May 2022 Revised: 18 August 2022 Accepted: 19 August 2022 Published: 30 September 2022

Abstract

Background: Impaired glucose regulation (IGR) represents the prediabetic state and is associated with gut microbiota (GM) dysbiosis and chronic inflammation. Tangning Ziyabitusi Tablet (TZT) is a Chinese Uyghur herbal medicine with preventative and therapeutic effects on diabetes, but its hypoglycemic mechanisms are unclear. **Methods**: Thirty-six male Wistar rats were divided into the normal diet (ND) and IGR groups. The IGR group was given a high-fat diet (HFD). After the IGR model establishment, the ND group was divided into ND and ND+TZT groups, and the IGR group into IGR and IGR+TZT groups. After 8 weeks of TZT administration, 16S rRNA sequencing and untargeted metabolomics were performed on fecal samples. Mesenteric lymph nodes were also collected, and T lymphocytes separated after rats were sacrificed. Flow cytometry was used to characterize different $CD4^+$ T cell subsets in mesenteric lymph nodes. Finally, we analyzed the correlation between GM and characteristic fecal metabolites. **Results**: Impaired glucose tolerance and insulin resistance were improved in the IGR+TZT group when compared with the IGR group. Bacterial 16S rRNA sequencing results showed that Sobs and Chao1 indices in the IGR group were significantly decreased, but were increased in the IGR+TZT group. The relative abundance of *Bacteroidetes* was decreased while the relative abundance of *Firmicutes* was increased in the IGR group. *Adlercreutzia* abundance was decreased after TZT administration, while the abundance of *Christensenellaceae_R-7_group*, *norank_f_norank_o_Clostridia_UCG-014*, *UCG-005*, and *Eubacterium_nodatum_group* was increased in the IGR+TZT group. Lymph node $CD4^+$ T cell proportions in the IGR group were significantly increased, while they were significantly decreased in the IGR+TZT group. Correlation analysis showed that tumor necrosis factor-α, interleukin-6, T helper cells (Th1, Th2, Treg), and insulin had a greater impact on GM community structure. **Conclusions**: TZT improved glucose tolerance and ameliorated GM dysbiosis in IGR rats. Additionally, TZT significantly modulated $CD4^+$ T cell subset proportions in rat mesenteric lymph nodes and fecal metabolism. Moreover, correlation analysis showed that key microbiota was closely related to IGR indices. Thus, TZT modulated GM composition and immune functions of the intestinal mucosa. We provide useful information for the investigation of active mechanisms and the clinical application of TZT.

Keywords: impaired glucose regulation; gut microbiota; Tangning Ziyabitusi Tablet; T lymphocyte subsets; metabolomics

1. Introduction

Impaired glucose regulation (IGR) is a pre-diabetes state and includes impaired fasting glucose (IFG) and impaired glucose tolerance (IGT) [1]. According to diagnostic criteria from the American Diabetes Association in 2017, the prevalence of IGR in Chinese adults was 35.2%, which was much higher than the weighted prevalence of total diabetes at 11.2% [2]. According to recent statistics, approximately 70% of patients with IFG and IGT eventually develop diabetes [3]. Therefore, key stages of diabetes prevention and treatment should be assessed at the IGR stage, thus, it is important to effectively intervene at this stage to delay or reduce diabetes [4]. However, some clinical drugs such as biguanides cause mild to severe side effects. Therefore, the identification of Chinese herbal medicine agents to treat diabetes has attracted considerable research interest.

In recent years, the relationship between T2DM and gut microbiota (GM) has received increasing attention. GM is a symbiotic micro-ecosystem in the body and plays important role in regulating metabolism [5,6]. Allin *et al*. [7] reported that the IGR population had GM dysbiosis; *Clostridium spp*. abundance was significantly reduced, while *Ruminococcus* abundance was significantly increased, suggesting GM changes in IGR. Moreover, in our previous study [8], we showed that Sobs and Shannon indices of GM in the IGR population decreased significantly, while the Simpson index increased significantly when compared with the healthy population. The Sobs index refers to the number of operational taxonomic units (OTUs) observed, which can reflect the species richness. The Shannon index is used to describe the disorder and uncertainty that occur in individuals of a species, the higher the uncertainty reflects the higher the diversity. Simpson index represents the probability that the number of individuals obtained from two consecutive samplings from a community species belongs to the same species, and also can

indicate the diversity of the community. Therefore, studying the relationships between GM dysbiosis and IGR has important clinical significance for preventing and treating T2DM.

Not only are there more than 10^{14} microorganisms in the human intestine, but large numbers of immune cells and immune factors are also present [9]. Studies have shown that GM is closely related to intestinal mucosal and parenteral immunity [6,10,11]. It has been shown that, in T2DM, there is a chronic cytokine-mediated inflammation that activates the innate immune system. Patients with T2DM often have cellular immune disorders, including elevated $CD4^+$ lymphocytes, which are associated with elevated blood glucose levels and decreased insulin secretion capacity [12]. Insulin resistance and impaired beta-cell function are often already present in IGR [13]. Hyperglycemia can up regulate markers of chronic inflammation. T lymphocytes are important cellular components that regulate the human immune system, and GM and associated GM metabolites exert key regulatory effects on $CD4^+$ proportions and other cell subsets [14]. Therefore, the role of GM and associated metabolites on intestinal immune functions warrant an investigation. Therefore, for IGR therapy, in addition to anti-inflammatory treatments, the application of auxiliary microecological regulators to regulate the imbalanced intestinal microbiota is particularly important.

Recent studies reported that traditional Chinese herbal medicines such as berberine can regulate the compositional ratio of beneficial and harmful bacteria, inhibit inflammation caused by GM dysbiosis, and generate good results for the clinical treatment of T2DM [15–18]. Tangning Ziyabitusi Tablet (TZT) is a traditional herbal medicine formula composed of herbal medicine *Acorns*, *Frankincense*, *Bletilla striata*, *Pomegranate flowers*, *Eucalyptus vulgaris*, *Galangal*, *Tianzhu Huang*, etc. Studies have shown that *Acorns* and *Frankincense*, the main components of TZT, have certain therapeutic effects on diabetes [19,20]. Studies from humans have shown that among the 219 diabetic patients treated with TZT, 78 cases had their blood glucose reduced to 7 mmol/L, accounting for 36% of them recovered; the total number of hypoglycemic effective patients is 167 cases, accounting for 76%. TZT regulated liver and kidney function, reduced urine levels and body weight, and was effective in the clinical treatment of diabetes [21]. However, the exact mechanism and whether the hypoglycemic effect of TZT is regulated by GM remains unclear.

Therefore, we observed the antidiabetic effects of TZT in a high-fat diet (HFD)-induced IGR model in rats. We studied GM changes in response to TZT treatment and the potential link between GM and T cell subsets in mesenteric lymph nodes. Our study provides an increased understanding of the potential TZT mechanisms for diabetes attenuation.

2. Materials and Methods

2.1 Animals

Animal protocols were approved by the Animal Research Committee of Xinjiang Medical University (Urumqi, China). Specific pathogen-free (SPF) male Wistar rats were purchased from the Animal Experiment Center of Xinjiang Medical University and housed in a controlled environment (12 h light/dark cycle) with free access to water. All experiments were approved by the ethics committee of Xinjiang Medical University (Permit Number: IACUC-20201026-24). Experimental diets, comprising normal diet (ND) (10% calories from fat, 20% calories from protein, and 70% calories from carbohydrate, MD12031) and the HFD (45% calories from fat, 20% calories from protein, and 35% calories from carbohydrate, MD12032), were purchased from Jiangsu Medison Biomedical Technology Co. Ltd (Nanjing, China).

2.2 Establishing an IGR Rat Model and Drug Interventions

Male SPF Wistar rats (aged 6 weeks) were adapted to the laboratory environment by feeding an ND for one week before studies. At 7 weeks old, 36 rats were randomly divided into ND and IGR groups. The ND group was received normal diet and the IGR group was fed HFD for 14 weeks. From the 6th week, an oral glucose tolerance test (OGTT) was performed every 2 weeks. According to the American Diabetes Association diabetes diagnosis and classification criteria, a successful IGR rat model comprised: Fasting plasma glucose (FPG) 5.6–6.9 mmol/L or a 2 hour postprandial blood glucose (2 h PG) of 7.8–11.1 mmol/L.

The two groups were further divided into four groups: ND, ND+TZT, IGR, and IGR+TZT groups. TZT was purchased from the hospital of Kashgar traditional Uyghur medicine (new drug name M20040974, Kashgar, China) and was dissolved in distilled water and administered by daily intragastric gavage at 308 mg/kg body weight. This dose was safe according to our pre-experiment. An equal volume of distilled water was given to the ND group. Body weight and food intake were measured weekly. After 8 weeks of intragastric administration, rats were anesthetized using 2.5% sodium pentobarbital (2 g/kg body weight) after 12 h starvation and humanely sacrificed by cardiac puncture. Blood was collected and serum separated by centrifugation. Organs and tissues were collected, weighed, and frozen at –80 °C.

2.3 Oral Glucose and Insulin Tolerance Tests (ITT)

For OGTT, rats were fasted for 12 h after which blood glucose was measured using the tail clipping method, and followed by gavage with distilled water or 50% glucose at 2 g/kg body weight. Blood glucose levels were measured at indicated time point. For ITT, rats were fasted for 6 h during the light cycle. Distilled water or insulin (INS) (recombinant human insulin, Solarbio, Beijing, China, 0.75 units/kg) was injected intraperitoneally, and blood glu-

cose levels were assayed at indicated time points after insulin injection. Blood glucose levels were measured using Roche's Blood Glucose Meter and Test Strips (AUUC-CHEK Performa Zhuoyuejingcai Glucose Meter, Roche Diabetes Care GmbH, Mannheim, Germany).

2.4 Enzyme-Linked Immunosorbent Assay (ELISA) Analysis

Serum INS, interleukin-2 (IL-2), tumor necrosis factor (TNF-α), and interleukin-6 (IL-6) levels were measured using ELISA kits (Elabscience, Wuhan, China) according to the manufacturer's instructions.

2.5 GM 16S rRNA Sequencing and Data Analysis

Fecal samples were randomly selected from groups (n = 6/group). DNA quality, after using a bacterial gDNA stool extraction kit (Qiagen, Hilden, Germany), was visually assessed by 1% agarose gel electrophoresis. We used the V3-V4 hypervariable region of *16S rRNA* and barcoded universal primers (forward 338F: 5′-ACTCCTACGGGAGGCAGCAG-3′; reverse 806R: 5′-GGACTACHVGGGTWTCTAAT-3′) to amplify DNA. Next, sequencing libraries were generated using TruSeq DNA PCR-free sample preparation kits (QIAGEN, USA). After assessing DNA quality, the library was sequenced using the Illumina MiSeq platform, with a sequencing length of 300 base pair (bp) paired-end reads (Shanghai Majorbio Bio-Pharm Technology, Shanghai, China).

We used fastp [22] (https://github.com/OpenGene/fastp, version 0.20.0) software for the quality control of raw sequencing sequences, and FLASH [23] (http://www.cbcb.umd.edu/software/flash, version 1.2.7) software for splicing. Sequences were aligned using the Silva database of bacterial *16S rRNA* (http://www.arb-silva.de) at a 70% confidence level using VSEARCH software. Operational taxonomic units (OTUs) were identified as one cluster at the 97% similarity level. Using UPARSE software [24] (http://drive5.com/uparse/, version 7.1), sequences were OTU clustered according to 97% similarity [24]. Subsequently, Mothur software (v1.35.1, http://www.mothur.org/) was used for rarefaction curve analysis, and α-diversity analyses containing an abundance-based coverage estimator and the Shannon index were performed. β-diversity analysis of the weighted unifrac distance matrix including principal component analysis (PCA) was conducted, while principal coordinate analysis (PCoA) was performed using Quantitative Insights Into Microbial Ecology (QIIME, v1.8.0, http://qiime.org). The relative abundance of bacteria in groups was calculated using the Wilcoxon rank-sum test. Linear discriminant analysis (LDA) effect size (LEfSe) was used to select biomarkers in different groups at LDA >4.0.

2.6 Flow Cytometry

Rat mesenteric lymph nodes were collected and grounded, and grounded liquid was filtered through a 200-mesh nylon mesh into a 15 mL centrifuge tube, centrifuged at 1500 rpm for 5 min to collect the cells, and the supernatant was discarded; an appropriate volume of PBS was taken to resuspend the cell pellet, and filtered through a 200-mesh nylon mesh into a new 15 mL centrifuge tube to prepare single cell suspension. Fluorescently conjugated antibodies fluoresce in isothiocyanate (FITC)-anti-CD4PE-anti-CD25 and Allophycocyanin, (APC)-anti-FOXP3 were used to label cells, while flow cytometry was used to detect Treg ($CD4^+CD25^+Foxp3^+0$) cells which accounted for the proportion of $CD4^+$ T lymphocytes. PerCP-Cy5.5-anti-CD3, FITC-anti-CD8, and PE-anti-IFN-γ were used to label cells, while flow cytometry was used to detect Th1 ($CD3^+CD8$-IFN-γ^+) cells which accounted for the proportion of $CD3^+$ T cells. PerCP-Cy5.5-anti-CD3, FITC-anti-CD8, and PE-anti-IL-4 were used to label cells, and flow cytometry was used to detect Th2 ($CD3^+CD8$-IL-4^+) cells as a percentage of $CD3^+$ T cells.

2.7 LC-MS Fecal Metabolomics Analysis

Frozen stool samples were thawed at 4 °C and untargeted fecal metabolomics analyses based on LC-MS were performed according to our previous study [25].

2.8 Statistical Analysis

Statistical analysis was performed in GraphPad Prism 8.0 (GraphPad Software, San Diego, CA, USA). Data was presented as the mean ± standard deviation. Unpaired two-tailed Student's *t* tests were used to compare two groups. When comparing multiple groups, one-way analysis of variance was used. Pearson correlation analysis between the altered fecal microbiota, environmental factors, and fecal metabolites. A $p < 0.05$ value was considered significantly different.

3. Results

3.1 Establishing a Rat IGR Model

The average body weight of the IGR group was significantly higher than the ND group after 4 weeks of feeding (Fig. 1A). Glucose tolerance was impaired in the IGR group after 14 weeks (Fig. 1B,C) and insulin resistance developed at week 15 (Fig. 1D,E). Therefore, a rat IGR model was successfully established according to ADA criteria.

3.2 TZT Attenuates HFD-Induced IGR and Dysfunctional Glucose Homeostasis in the IGR Rat Model

To evaluate the antidiabetic effects of TZT, rats in the IGR group were administered 308 mg/kg/day TZT or vehicle by gavage for 8 weeks, starting from 7 weeks old. The HFD increased body weight when compared with ND-fed animals (Fig. 2A). In contrast, TZT administration attenuated body weight gain in IGR rats (Fig. 2A). OGTT results showed that IGT in the IGR+TZT group was improved when compared with the IGR group (Fig. 2B,C), and ITT data showed that insulin resistance was improved

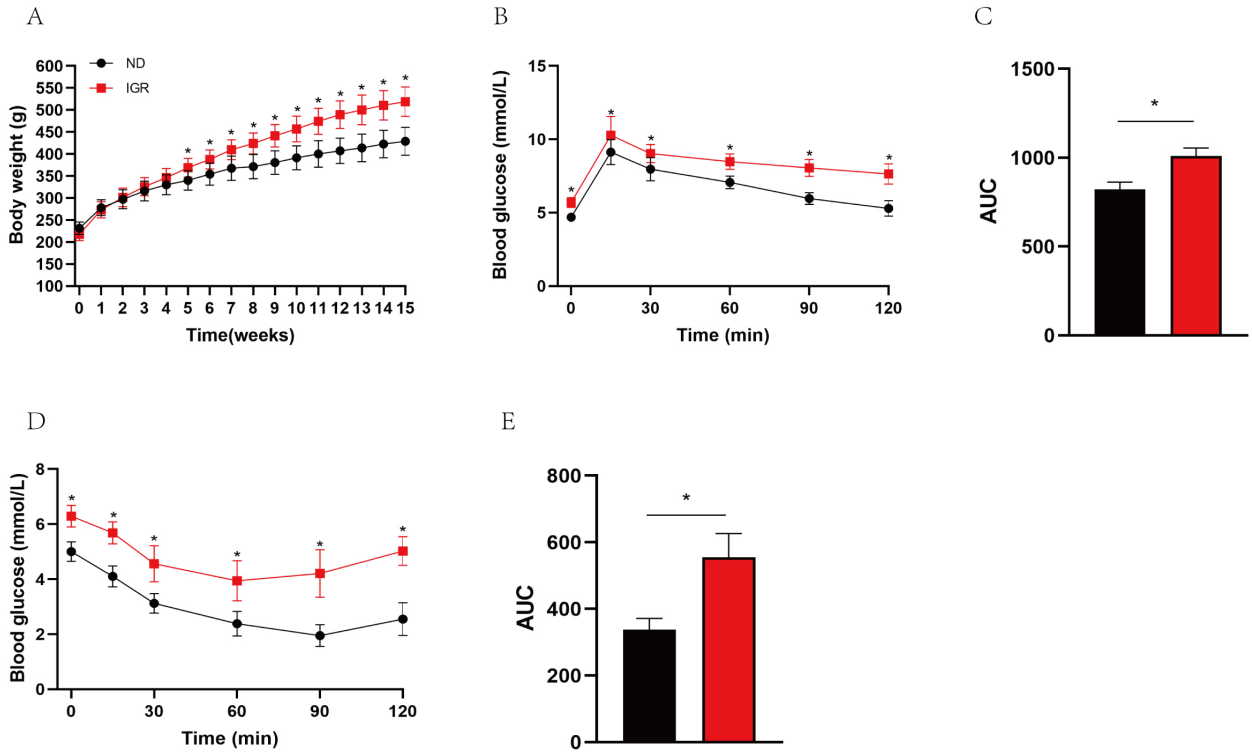

Fig. 1. Establishment of a rat IGR model. (A) Body weight change in the ND and IGR groups. (B–C) Result of OGTT after 14 weeks in the ND and IGR groups. (D–E) Result of ITT after 15 weeks in ND and IGR groups (n = 6/group).

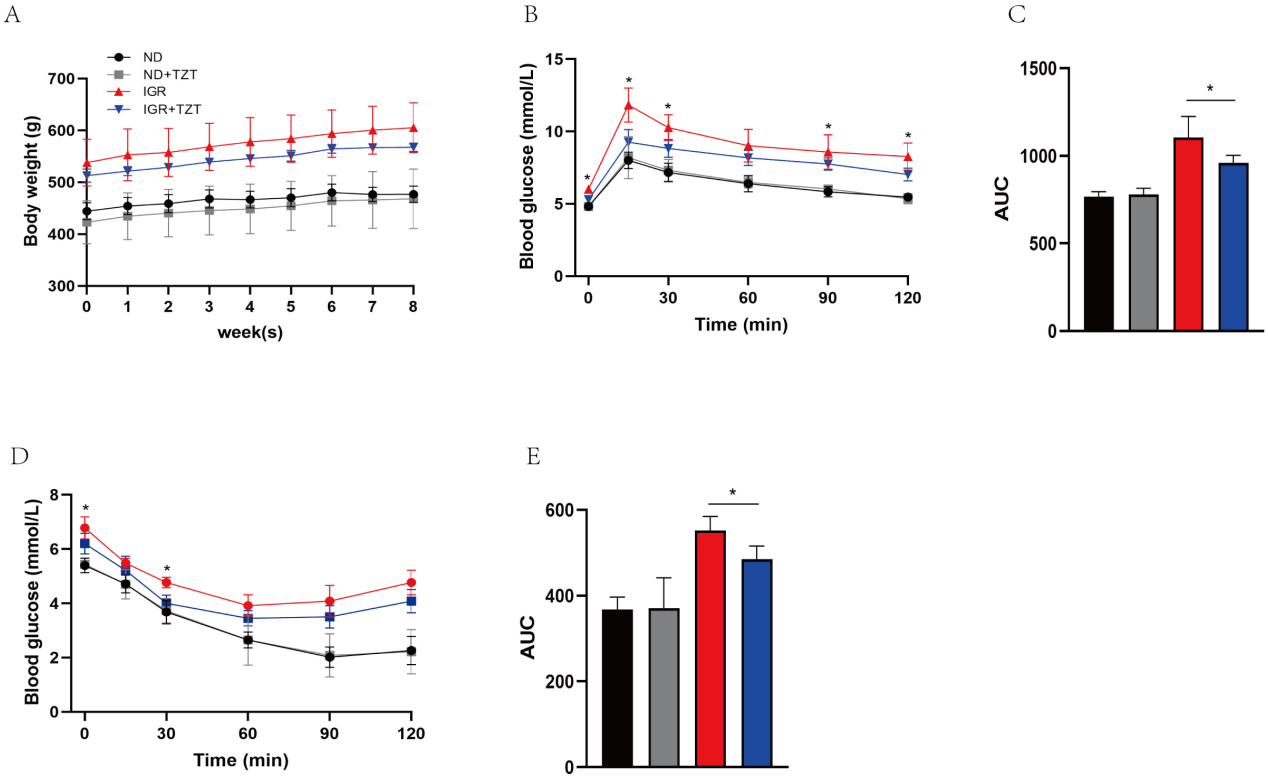

Fig. 2. The effects of TZT on plasma glucose and insulin levels in IGR rats. (A) Body weight over the 8-week of TZT intervention. (B–C) PG levels at 2 h were tested by OGTT after 8-week intervention. (D–E) Insulin level were tested by ITT after 8-week intervention (n = 6/group).

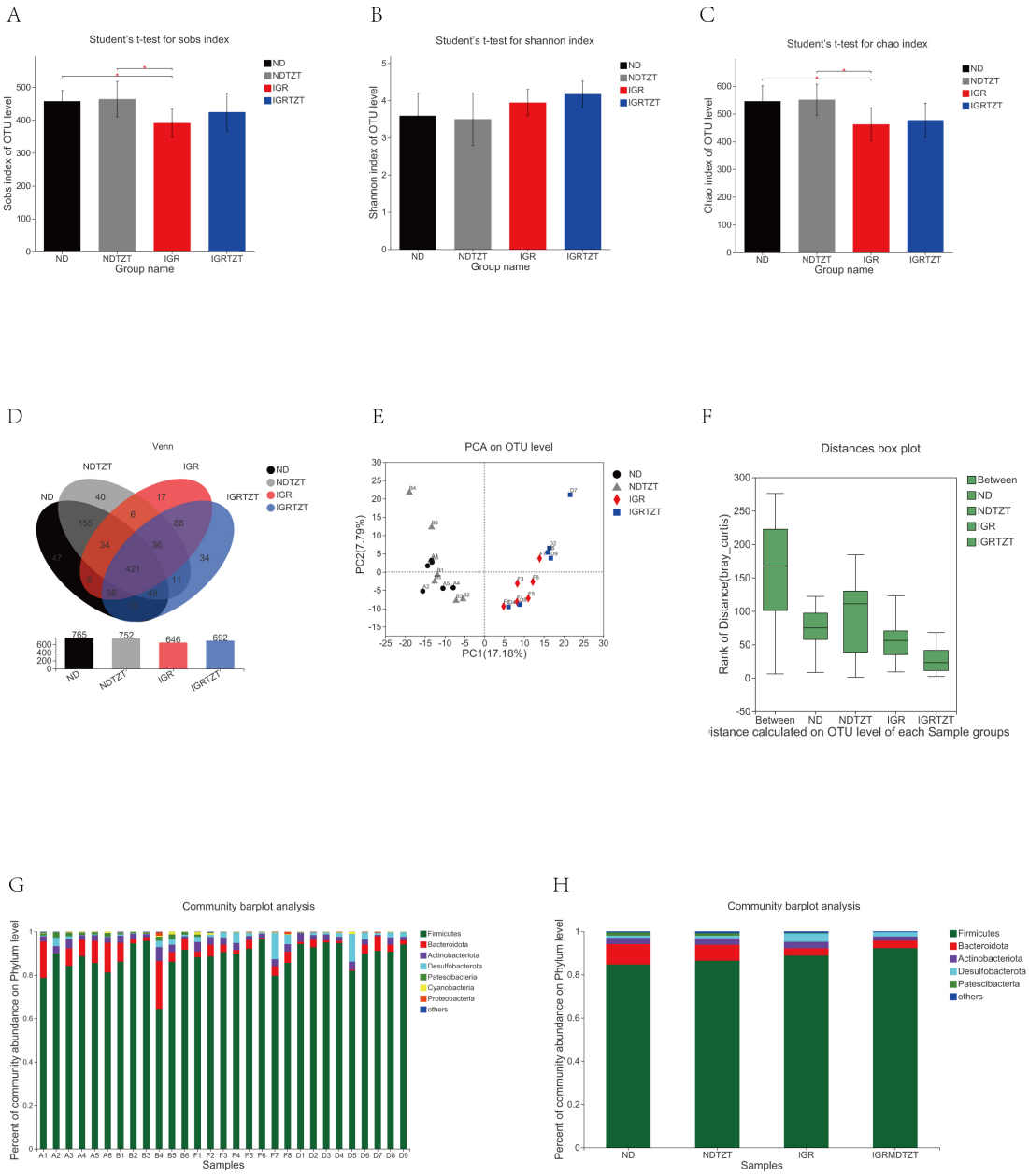

Fig. 3. The effects of TZT on gut microbial abundance and diversity in IGR rats. (A) Sobs index. (B) Shannon index. (C) Chao1 index. (D) Venn diagram analysis. (E) OTU distance-based PCA, and weighted unifrac-based PCoA (F) ANOSIM analysis. (G–H) A histogram of relative bacterial abundance at the phylum level.

in the IGR+TZT group when compared with the IGR group (Fig. 2D,E). Thus, TZT administration attenuated HFD-induced IGR and insulin resistance.

3.3 TZT Modulates GM Diversity and Composition in HFD-Induced IGR Rats

Bacterial *16S rRNA* sequencing, based on the V3-V4 hypervariable region, was used to analyze the effects of TZT on GM dysbiosis in IGR rats. An average of 63,436 raw reads were generated from each sample. After removing low-quality sequences, 57,928 optimized sequences were analyzed and clustered into OTUs (**Supplementary Table 1**); the average length of an optimized sequence was 412 bp. Rarefaction analysis showed the sequencing depth covered rare and new phylotypes and most bacterial diversity (**Supplementary Fig. 1**). In total, 12 phyla, 210 genera, 371 species, and 989 OTUs were generated. α-diversity analysis showed a significant decrease in bacterial diversity in the IGR group and increased diversity in response to TZT therapy. When compared with the ND group, the Sobs index of the IGR group was significantly decreased ($p < 0.05$, Fig. 3A). When compared with the IGR group, the Sobs index increased in the IGR+TZT group, but it was not statistically different. Also, the Shan-

non index showed that when compared with the IGR group, IGR+TZT group diversity was increased, but not statistically significant (Fig. 3B). The Chao1 index showed that when compared with the ND group, microbiota richness in the IGR group was decreased, while the Chao1 index of the IGR+TZT group was increased (Fig. 3C).

From the Venn diagram analysis, 421 common OTUs were identified in the four groups, but OTUs in IGR and IGR+TZT groups were <ND and ND+TZT groups. OTUs in the IGR+TZT group were >the IGR group (Fig. 3D).

To further investigate overall differences in β-diversity, structural changes in GM were assessed using OTU distance-based PCA and weighted unifrac-based PCoA. As shown (Fig. 3E, **Supplementary Figs. 2,3**), microbiota clustering was significantly different between the ND and IGR groups, but the ND+TZT group showed a similar structure to the ND group, whereas the IGR+TZT group had a different structure to the corresponding IGR group. In addition, analysis of similarities (ANOSIM) identified GM differences among the four groups (r = 0.7008, p = 0.001, Fig. 3F and **Supplementary Table 2**). Inter-group differences in GM composition in the IGR and IGR+TZT groups were >intra-group differences, and composition differences in ND and ND+TZT groups were similar between the two groups. As indicated (Fig. 3G,H) phylum-level analysis showed that the relative abundance of *Bacteroidetes* decreased and the relative abundance of *Firmicutes* increased in the IGR group when compared with the ND group.

To examine the effects of TZT on gut microbial composition in IGR rats, we analyzed the relative abundance of gut bacteria at phylum and genus levels. The abundance of *Patescibacteria*, *Verrucomicrobiota,* and *Elusimicrobiota* was statistically different in the four groups at phylum levels. When compared to the ND and ND+TZT groups, *Patescibacteria* and *Elusimicrobiota* were decreased in the IGR and IGR+TZT groups (Fig. 4A). When compared to the IGR group, *Verrucomicrobiota* was significantly decreased in the IGR+TZT group.

To further examine differences between samples, a genus level analysis was performed. As showed (Fig. 4B), the HFD decreased the relative abundance of *norank_f_norank_o_Clostridia_UCG-014,* whereas TZT reversed these alterations. The HFD increased the relative abundance of *Streptococcus*, *Ruminococcus_gauvreauii_group*, *norank_f_Lachnospiraceae*, *norank_f_Oscillospiraceae*, *Colidextribacter* and *Ruminococcus_torques_group*, whereas TZT reversed these alterations. When compared with the IGR group, the proportion of the genera, *Adlercreutzia*, *Parvibacter*, *Enterorhabdus*, *Akkermansia* and *Alloprevotella* were significantly decreased after gavage with TZT, and the proportion of *Christensenellaceae_R-7_group*, *norank_f_norank_o_Clostridia_UCG-014*, *UCG-005*, *Eubacterium_nodatum_group*, *Family_XIII_AD3011_group*, *norank_f_Christensenellaceae*, *Allobaculum*, *Marvinbryantia*, *Hungatella*, and *Globicatella* was increased (Fig. 4C).

LEfSe was used to perform multi-level species difference LDA based on taxonomic composition in the four groups (Fig. 4D,E). In the *Firmicutes* phylum, *Lactobacillus* and *Monoglobus* genera were over-represented in the ND group. The *norank_f_norank_o_Clostridia_UCG-014* genus was more abundant in the ND+TZT group. The *norank_f_Lachnospirales*, *Streptococcaceae*, *Ruminococcus_gauvreauii_group*, *Colidextribacter*, *norank_f_Oscillospiraceae* and *Ruminococcus_torques_group* genera were more abundant in the IGR group. The abundance of *unclassified_f_Lachnospiraceae*, *Blautia*, *Christensenellaceae_R-7_group*, and *Lachnoclostridium* genera was higher in the IGR+TZT group.

3.4 TZT Regulates CD4$^+$ T Cell Proportions in Rat Mesenteric Lymph Nodes

When compared with the ND group, the lymph node CD4$^+$ ratio in the IGR group was significantly increased, while in the IGR+TZT group it was significantly decreased ($p < 0.05$). This suggested that TZT exerted significant regulatory effects on CD4$^+$ lymphocytes (Fig. 5A,B). When compared with the ND group, Th1 cells in the IGR group were significantly decreased, but no significant changes were observed in the IGR+TZT group (Fig. 5C,D). When compared with the ND group, Th2 cells in the IGR group were significantly decreased, while in the IGR+TZT group, they were significantly increased (Fig. 5E,F). When compared with the ND group, Treg cells in the IGR group were significantly increased. When compared with the IGR group, no significant change was observed in the IGR+TZT group, suggesting TZT had no significant regulatory effect on Treg cells (Fig. 5G,H).

3.5 The Correlation Analysis between Altered Microbiota and Serum Parameters

Redundancy analysis (RDA) and Canonical correspondence analysis (CCA) were used to identify relationships between environmental factors and microbial composition. Environmental factors included serum INS, IL-2, TNF-α, IL-6, FPG, 2 h PG, CD4$^+$ T cell subsets, Th1, Th2, and Treg cells. We observed that Tregs, IL-6 ($p < 0.05$), INS, and FPG had a greater impact on bacteria phylum structures (Fig. 6A). *Campilobacterota* abundance was negatively correlated with FPG, *Elusimicrobiota* abundance was positively correlated with TNF-α, IL-2, Th1, and Th2, and negatively correlated with FPG, 2 h PG, INS, and Tregs. *Proteobacteria* abundance was negatively correlated with FPG, 2 h PG, Tregs, and positively correlated with Th1. *Patescibacteria* abundance was negatively correlated with FPG, 2 h PG, INS, and Tregs, and positively correlated with TNF-α and Th1. *Desulfobacterota* abundance was positively correlated with FPG, 2 h PG, and Tregs,

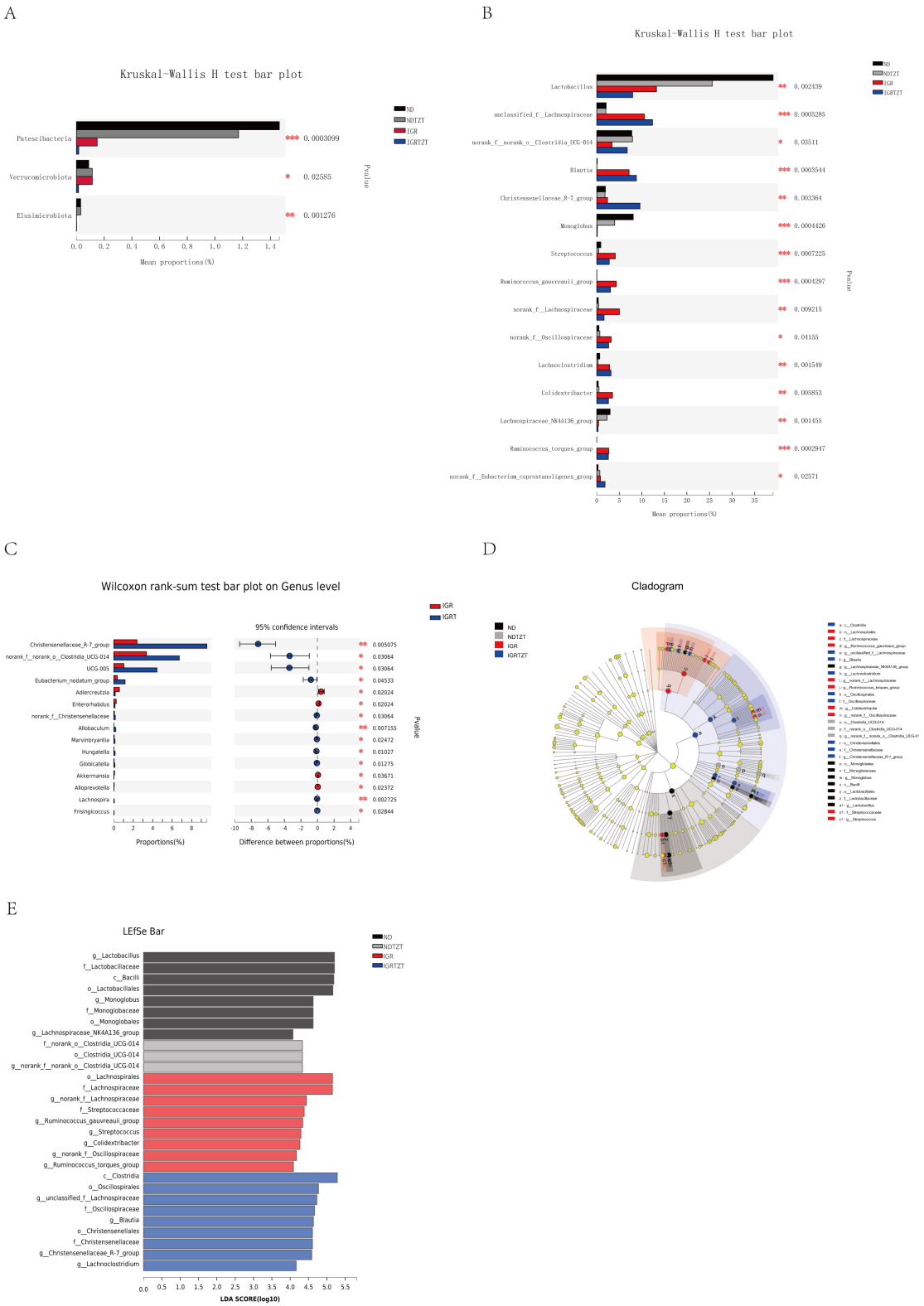

Fig. 4. β-diversity analysis of gut microbiota in four groups. (A) Kruskal-Wallis H test bar plot at the phylum level. (B) Kruskal-Wallis H test bar plot at the genus level. (C) Wilcoxon rank-sum test bar plot at the genus level between the IGR and IGR+TZT groups. (D) Lefse analysis: the cladogram shows microbial species with significant differences in the ND (black), ND+TZT (gray), IGR (red), and IGR+TZT (blue) groups. Species classification at phylum, class, order, family, and genus levels is shown from the inside to the outside. Red, blue, and black nodes in the phylogenetic tree represent differential microbial species in different groups. Yellow nodes represent species with no significant differences. (E) Linear discriminative analysis (LDA) effect size (LEfSe) among groups. Species with significant differences have an LDA score >4.0. The histogram length represents the LDA score.

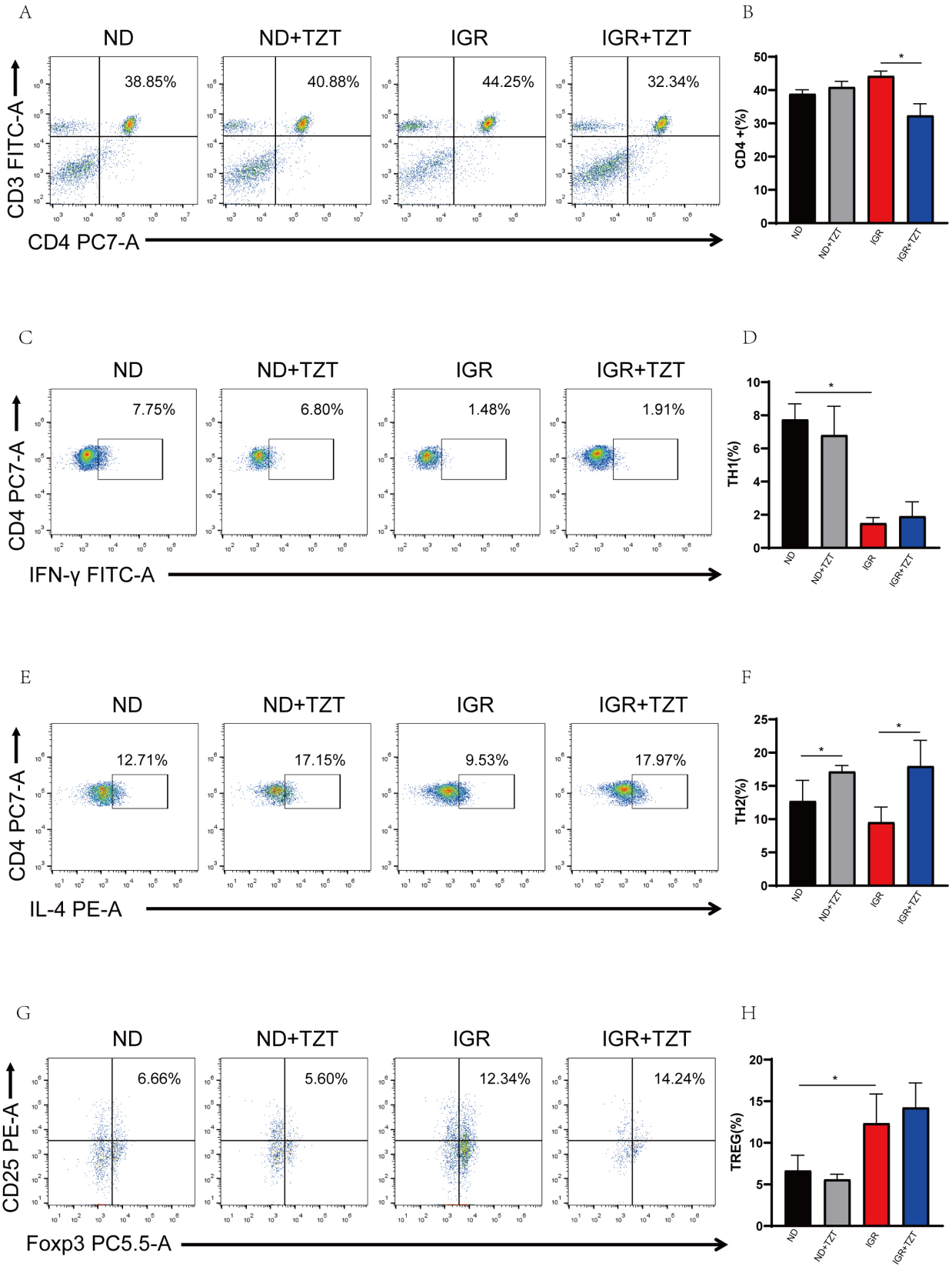

Fig. 5. TZT modulates CD4+ T cell subset proportions in rat mesenteric lymph nodes. (A–B) The proportion of CD4+ T cell subsets in mesenteric lymph nodes in the four groups. (C–D) The proportion of Th1 cell subsets in mesenteric lymph nodes of the four groups. (E–F) The proportion of Th2 cell subsets in mesenteric lymph nodes in the four groups. (G–H) The proportion of Treg cell subsets in the mesenteric lymph nodes in the four groups (n = 6/group).

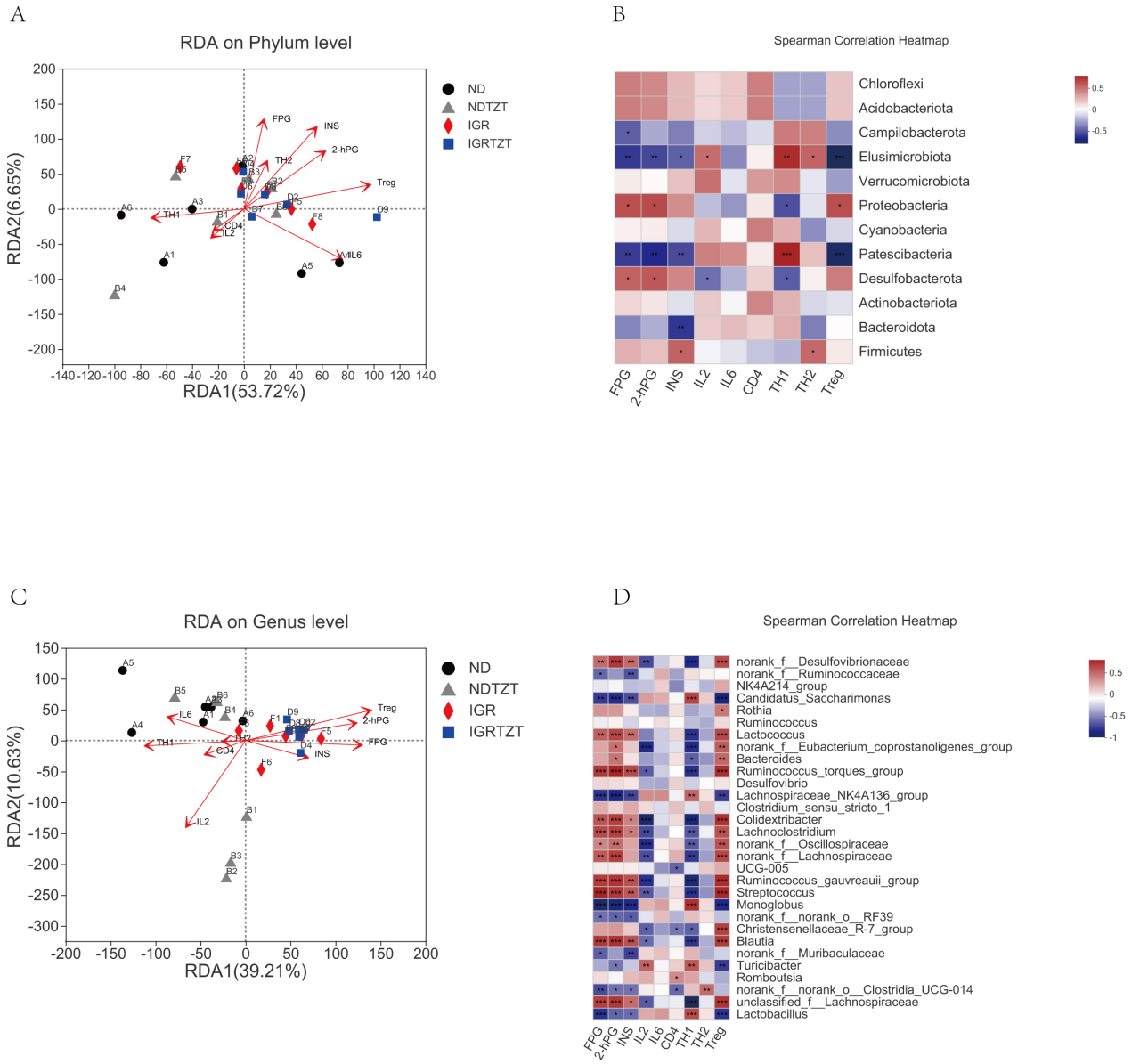

Fig. 6. Pearson correlation analyses between alternated microbiota, serum parameters, and T cell subsets. (A) RDA analysis at the phylum level. (B) Spearman correlation heatmap at the phylum level. (C) RDA analysis at the genus level. (D) Spearman correlation heatmap at the genus level.

and negatively correlated with IL-2 and Th1. *Bacteroidota* abundance was negatively correlated with INS and Th2 and positively correlated with TNF-α. *Firmicutes* abundance was negatively correlated with Th1 (Fig. 6B).

Treg ($p < 0.05$), 2 h PG, and INS levels had a greater impact on microbiota genus structures (Fig. 6C). Heatmap analysis showed that IL-2, $CD4^+$, and Th1 levels were negatively correlated with *Christensenellaceae_R-7_group*, while Tregs were positively correlated with *Christensenellaceae_R-7_group*. FPG, 2 h PG, INS, and $CD4^+$ were negatively correlated with *norank_f__norank_o__Clostridia_UCG-014*, while Th2 was positively correlated with *norank_f__norank_o__Clostridia_UCG-014*. *UCG-005* was negatively correlated with $CD4^+$ (Fig. 6D).

3.6 TZT Restores Perturbed Fecal Metabolites in IGR Rats

LC-MS fecal metabolomics analysis was used to identify different metabolomics features in the four groups. Both PCA and orthogonal partial least-squares discrimination analysis (OPLS-DA) score plots showed significant differences between groups, indicating that a different glycemic status exerted different fecal metabolomics profiles (Fig. 7A,B). Permutation testing showed no overfitting data and validated the partial least-squares discrimination analysis (PLS-DA) model (**Supplementary Fig. 4**). To reflect variations between group samples and overall metabolic differences between groups, PCA was performed

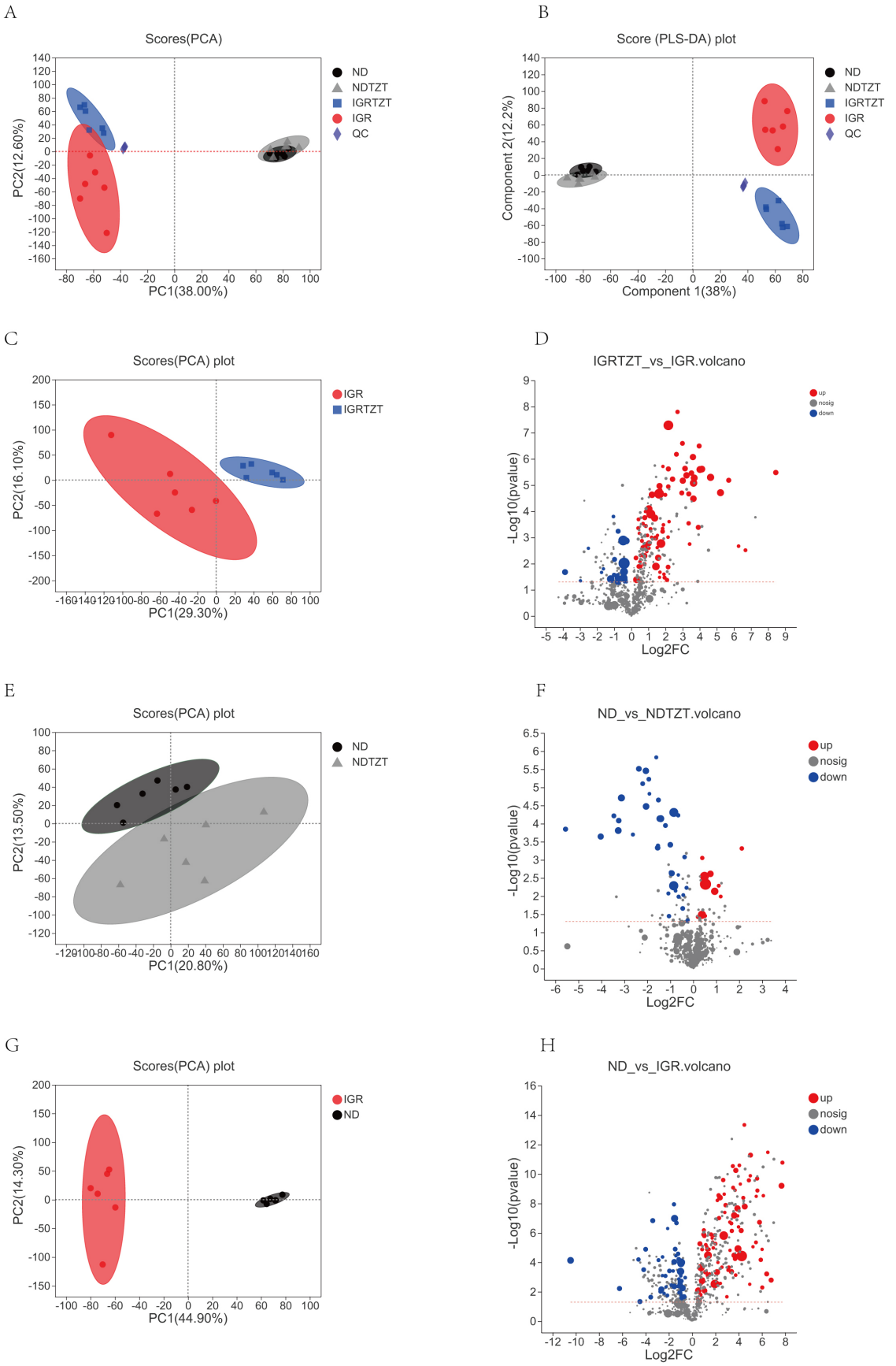

Fig. 7. Fecal metabolomics analysis. (A–B) PCA and OPLS-DA analyses. (C–D) PCA analysis between the IGR and IGR+TZT groups. (E–F) PCA analysis between the ND and ND+TZT groups. (G–H) PCA analysis between the IGR and ND groups.

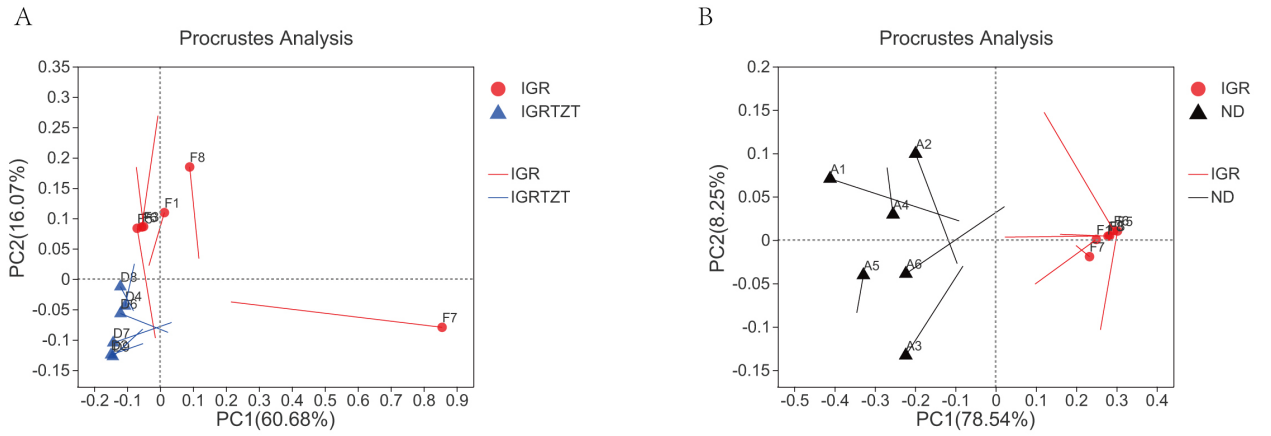

Fig. 8. Procrustes analysis. (A) Procrustes analysis between the IGR vs. IGR+TZT group. (B) Procrustes analysis between the ND vs. IGR group.

for ND vs. ND+TZT, IGR vs. IGR+TZT, and ND vs. IGR. The PCA score plot showed the partitioning trend between ND and IGR group samples was obvious, and partitioning trends between IGR and IGR+TZT group samples were also obvious. These observations suggested that fecal metabolites in IGR animals changed and that fecal metabolites were also altered after TZT (Fig. 7C–H).

3.7 Integrated Analysis of GM and Fecal Metabolomics

To explore gut flora species that were significantly associated with potential metabolites, an integrated analysis of metabolomics and metagenomics was performed in groups. Firstly, a Procrustes analysis was performed to assess data consistency from the gut microbiome and fecal metabolomics profiling; the similarity between the two datasets was low although significance was identified between the IGR vs. IGR+TZT groups and ND vs. IGR groups ($p < 0.01$, Fig. 8A,B).

LC-MS metabolomics analyses identified 21 differentially enriched metabolites between the four groups (Fig. 9A).

Next, we analyzed possible correlations between altered fecal metabolites and microbial phylum or genus using Spearman's correlation analysis. Correlation analyses at the phylum level (Fig. 9B,C) showed that metabolite M6 content in feces was positively correlated with *Cyanobacteria* ($r = 0.490$), *Patescibacteria* ($r = 0.128$), and *Actinobacteriota* ($r = 0.659$). Alpha-muricholic acid, cholic acid, and taurine were positively correlated with *Desulfobacterota* ($r = 0.611$, $r = 0.657$, and $r = 0.620$, respectively). Multiple metabolites were positively correlated with *Campilobacterota*, while pregnanediol was negatively correlated with *Campilobacterota* ($r = –0534$). Asteltoxin, guanine, and deoxyguanosine were negatively correlated with *Bacteroidota* ($r = –0.510$, $r = –0.533$, and $r = –0.529$, respectively). Pregnenolone was negatively correlated with *Actinobacteriota* ($r = –0.623$).

At the genus level, *Adlercreutzia* was negatively correlated with megaphone (r = –0.488), 11-dehydro-thromboxanw B (TXB) ($r = –0.491$), camellenodiol ($r = –0.601$), perulactone ($r = –0.503$), lucyin A ($r = –0.511$), and pregnenolone ($r = –0.486$). *Christensenellaceae_R-7_group* was positively correlated with 21-β-hydroxyhederagenin ($r = 0.489$), PG (17:0/0:0) ($r = 0.546$), and pregnenolone ($r = 0.556$). *UCG-005* was positively correlated with PG (17:0/0:0) ($r = 0.486$), 14-β-hydroxyyohimbine ($r = 0.488$), estrane-3-α,17-α-diol ($r = 0.493$), farnesyl acetone ($r = 0.486$), methandriol ($r = 0.537$), and 3beta,5alpha,6alpha,7beta,14alpha,22E,24R)-5,6-epoxyergosta-8,22-diene-3,7,14-t ($r = 0.732$), and negatively correlated with 1-oxoprevitamin D3 ($r = –0.490$). *Eubacterium_nodatum_group* was positively correlated with 3beta,5alpha,6alpha,7beta,14alpha,22E,24R)-5,6-epoxyergosta-8,22-diene-3,7,14-t (r = 0.558) and farnesyl acetone ($r = 0.530$) (Fig. 9D).

Kyoto Encyclopedia of Genes and Genomes pathway enrichment and pathway topology analysis were performed. Based on metabolite changes between IGR and IGR+TZT groups, five metabolic pathways exerted a high impact and included, tryptophan metabolism, retinol metabolism, taurine, and hypotaurine metabolism, brassinosteroid biosynthesis, and steroid hormone biosynthesis (Fig. 10).

In summary, by combining GM phylum and genus associations with fecal metabolites, *Patescibacteria*, *Verrucomicrobiota*, *Bacteroidota*, *Actinobacteriota* and their associated metabolites α-muricholic acid, cholic acid, metabolite M6, asteltoxin, guanine, deoxyguanosine, and pregnenolone were involved in antidiabetic effects mediated by TZT in IGR rats.

4. Discussion

T2DM is a complex polygenic genetic disease and is generated by the combined actions of genetic and environmental factors [26]. In recent years, the relationship be-

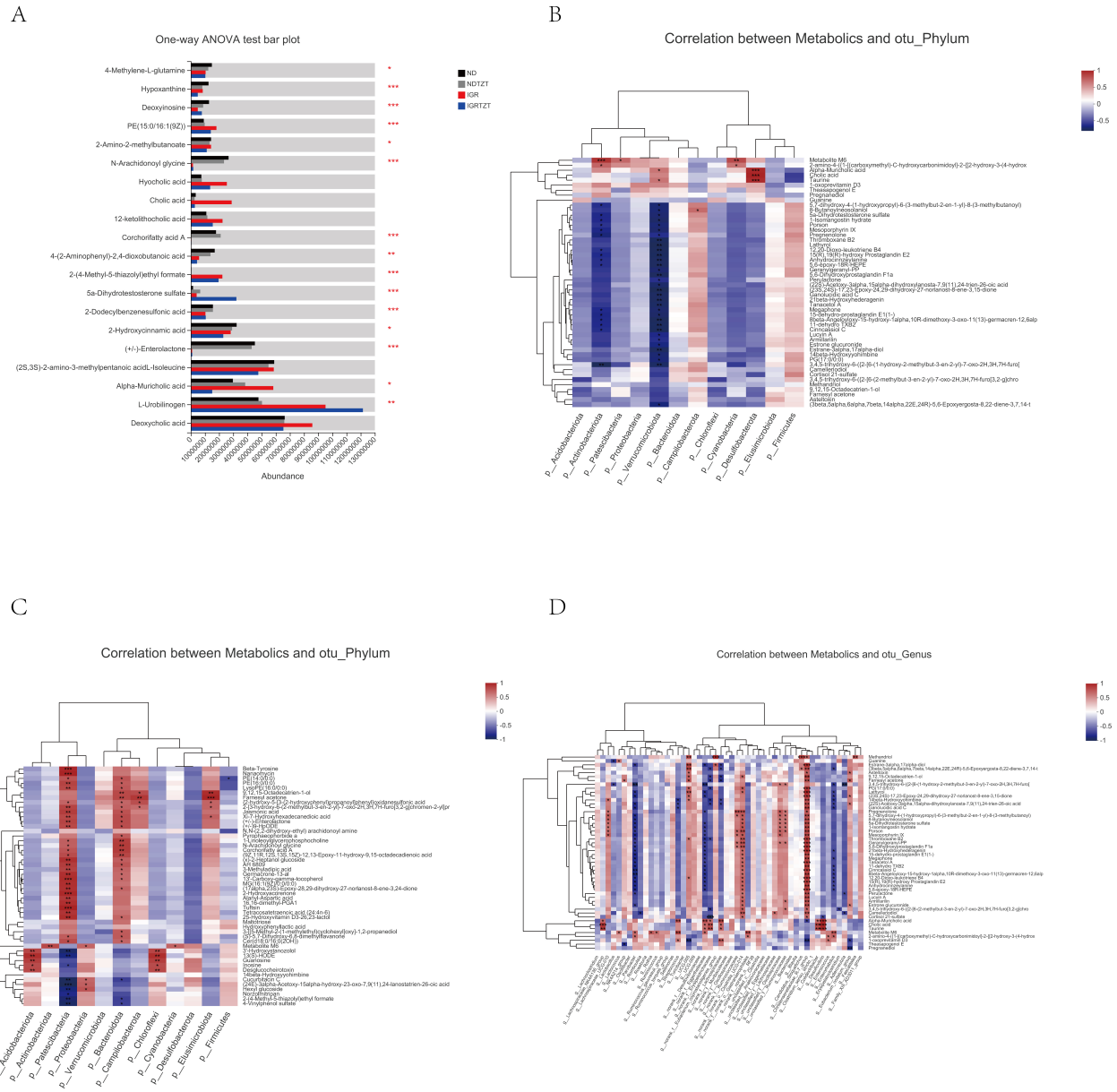

Fig. 9. Correlation analyses between alternated microbiota and alternated fecal metabolites. (A–B) Correlation between fecal metabolic and microbial phylum. (C–D) Correlations between fecal metabolic and genus.

tween T2DM and GM has become a topical research field. The GM inhabit the gut and are symbiotic with the host, thus they affect the host body's metabolism and immune functions to varying degrees [27]. The gut's innate immune system is the first line of defense against different bacterial antigens. Species diversity is an important indicator of intestinal health as it helps maintain a balanced healthy gut. GM diversity is more abundant in healthy individuals, while it is lower in obese and T2DM individuals. In our study, community richness and the Sobs index were significantly decreased in the IGR group. When compared with this group, community and Sobs indices were increased in the IGR+TZT group which suggested that post TZT intervention, GM in IGR rats had become richer. Magne F *et al.* [28] showed that when compared with healthy individuals, the *Firmicutes* to *Bacteroidetes* ratio was increased in obese and diabetic patients, while in a probiotic supplemented population, the *Bacillus perfringens* (*Firmicutes* representative) to *Bacteroides fragilis* (*Bacteroidetes* representative) ratio was significantly reduced [29–31]. In our study, when compared with the ND group, *Firmicutes* and *Bacteroidetes* ratios were also increased in IGR rats and suggested GM dysbiosis at the IGR stage.

The relative abundance of *Patescibacteria* and *Elusimicrobiota* at the phylum level decreased in the IGR group, and *Verrucomicrobiota* abundance decreased following TZT exposure. We found that *Patescibacteria* abundance decreased in the HFD-induced IGR group,

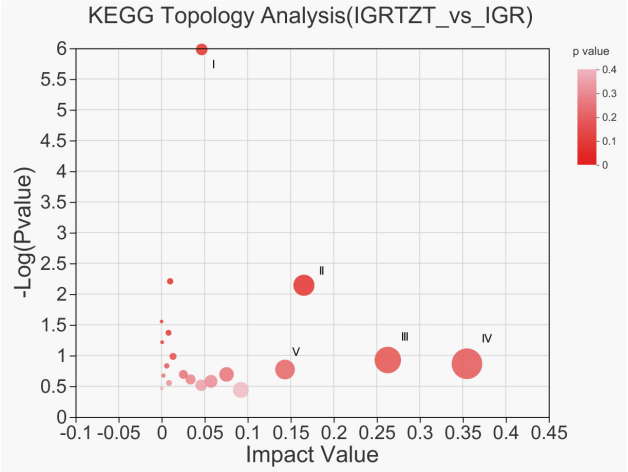

Fig. 10. Topology analysis of metabolic pathways between the IGR and IGR+TZT groups. The X-axis represents the pathway impact and the Y-axis represents pathway enrichment. Larger sizes and darker colors represent greater pathway enrichment and higher pathway impact values. I: Steroid hormone biosynthesis; II: Tryptophan metabolism; III: retinol metabolism; IV: taurine and hypotaurine metabolism; V: brassinosteroid biosynthesis. * $p < 0.05$, ** $p < 0.01$, *** $p < 0.001$.

consistent with Lu *et al*. [32]. Also, *Patescibacteria* was negatively correlated with FPG, 2 h PG, INS, and Tregs, and positively correlated with Th1 and TNF-α levels. The study showed that reducing the number of *Patescibacteria* was connected with the indicators of alcoholic fatty liver (AST, TG, etc.), but the abundance of the bacterial didn't reach the statistical difference between the control and alcoholic fatty liver model group [33]. As yet, little is known about the ecology and evolution of *Patescibacteria*, particularly concerning how they might interact with other taxa [34]. Some microbiota genus belonging to *Patescibacteria* may be beneficial to human health, and some of them may be harmful. The function of specific bacterium belonging to in super-phylum is complex and largely unknown. Zhang, *et al*. [35] reported that decreased level of *Verrucomicrobia* has been suggested to be a potential marker for T2DM. *Verrucomicrobia* abundance decreased in IGR rats in this study, but it wasn't increased after TZT gavage. *Patescibacteria* and *Verrucomicrobia* are the very super-phylum that includes many types of bacterial genera and species. Different bacteria genus or species in the same phylum may have different functions, and different herbal medicine may affect the same bacteria and produce different bacterial metabolites that can affect intestinal integrity and immunity. The controversial results need to be further investigated and we need to have more specific bacteria functional research to find the specific microbial marker of the metabolic disease. Lefse analysis showed that *Lachnospirales* abundance was higher in the IGR group. Ruuskanen *et al*. [36] showed that when compared with the normal population, the proportion of *Lachnospirales* in the fatty liver population was significantly higher and suggested that *Lachnospirales* may correlate with obesity and IGR. Also, *Oscillospiraceae* content was higher in the IGR+TZT group. Maya-Lucas *et al*. [37] reported that *Oscillospiraceae* levels in obese children were significantly lower than in normal children, and were negatively correlated with serum cholesterol levels. Thus, *Oscillospiraceae* may be a beneficial bacteria for obese and IGR populations. When compared with the IGR group, the proportion of the genus *Adlercreutzia* was significantly decreased after TZT administration, and the proportions of *Christensenellaceae_R-7_group*, *norank_f_norank_o_Clostridia_UCG-014*, *UCG-005*, and *Eubacterium_nodatum_group* genera were increased. Dekker Nitert *et al*. [38] showed that *Adlercreutzia* abundance was positively correlated with body mass index and serum leptin levels in humans, while in rodents, abundance was associated with obesity and insulin resistance, which is consistent with the *Adlercreutzia* was significantly elevated in the IGR group in this study, and TZT treatment decreased the abundance of *Adlercreutzia*. Wei *et al*. [39] reported that *Adlercreutzia* abundance decreased in a T2DM rat model after intervention with the traditional Chinese medicine Xiexin Tang. Gong *et al*. [40] showed that Chinese herbal anti-aging tablets reduced *Christensenellaceae_R-7_group* levels in obese mice, but in our study, *Christensenellaceae_R-7_group* abundance was increased in the IGR+TZT group. Li ZR *et al*. [41] showed that the Undaria pinnatifida polysaccharides (UPP) intervention significantly reduced FPG levels, alleviated insulin resistance, and improved glucose tolerance in diabetic rats. 16S rRNA analysis showed that gut microbiota composition altered after UPP intervention, resulting in elevated *Alistipes*, *Bacteroides*, and *Christensenellaceae_R-7_groups* abundance. In addition, Xie J *et al*. [42] showed that pectin and inulin can improve the integrity of the intestinal barrier to a certain extent by affecting the GM, the *Christensenellaceae_R-7_group* increased significantly after pectin and inulin intervention. The content so we considered Christensenellaceae_R-7_group as beneficial bacteria. Different Chinese herbal medicine ingredients have different effects on the same bacteria species, and different microbiota metabolites are produced after the intervention.

It was reported that beneficial bacteria belong to the *Ruminococcus UCG-005* family which is a key bacterium for diabetes prevention [43]. When compared with the IGR group, the IGR+TZT group significantly increased UCG-005 levels, which agreed with our assumption that TZT may increase the beneficial bacteria. Consistently, TZT ameliorated impaired glucose regulation by modulating GM composition. TZT treatment was highly correlated with *Oscillospiraceae*, *Adlercreutzia*, *Christensenellaceae_R-7_group*, *norank_f_norank_o_Clostridia_UCG-014*,

UCG-005, and *Eubacterium_nodatum_group* levels.

Several studies confirmed that GM is closely related to the immune system, intestinal mucosal immunity, and parenteral immunity [44,45]. Probiotics not only directly affect immune function but also indirectly regulate the immune state [10,11,46]. Studies have shown that $CD4^+$ T cells interact with GM in a complex and dynamic manner, and play important roles in coordinating adaptive and innate immune responses [47]. Wang *et al*. [12] showed that when compared with healthy individuals, $CD4^+$ T cell proportions in the peripheral blood of T2DM patients were increased, and bone marrow mesenchymal stem cells inhibited $CD4^+$ T cell activity and T2DM. This observation was consistent with our findings, such that $CD4^+$ T cells number in the mesenteric lymph nodes of IGR animals were significantly increased when compared with ND animals, whereas $CD4^+$ T numbers were significantly decreased in IGR+TZT animals, and suggested TZT may delay diabetes by down-regulating the proportion of $CD4^+$ T cells. The $CD4^+$ T cell subset is a mix of functionally distinct cell types including Th1, Th17, and regulatory T cells (Treg), etc, that can affect chronic inflammation. $CD4^+$ T cells influence obesity-associated inflammation, especially the systemic inflammation that provokes numerous obesity comorbidities in people. A recent study showed that $CD4^+$T cells from subjects with prediabetes produces a unique inflammatory profile [48]. A better understanding of $CD4^+$ T change in prediabetes is also important for clarifying the gut microbiota- host immunity interaction in metabolic disease. In this study, Treg increased in mesenteric lymph nodes of IGR rats. Treg counteracts inflammation, as demonstrated in insulin resistant animals [49,50]. Microbial metabolites regulate host immunity by exploiting metabolite-specific immune cell receptors such as G protein-coupled receptors (GPR41, GPR43, GPR109A), aryl hydrocarbon receptor (AhR), farnesoid X receptor (FXR), etc. [51]. These receptors, which play crucial roles in host-microbiota interactions, are expressed at various levels in different cell types such as intestinal epithelial cells (IECs), innate lymphoid cells, macrophages, T cells, and dendritic cells [52]. So, changed bacterial structural components and bacterial metabolites after TZT intervention either directly or indirectly (through increasing inflammatory mediators and regulating the intestinal mucosal immunity) impact and modulate the gut barrier functions in IGR. A better understanding changes of $CD4^+$ T cell subset in prediabetes is also important for clarifying the gut microbiota- intestinal mucosal immunity interaction in metabolic disease.

Interactions occur between the intestinal microbiota and the host immune system [53,54]. Using redundancy analysis (RDA)/canonical correspondence analysis (CCA) analysis, Tregs and INS had a considerable impact on microbiota phyla and genus abundance. Insulin resistance is a key characteristic of patients with IGR, so we hypothesize that different GM compositions in IGR may be related to INS content. At the phylum level, *Elusimicrobiota*, *Proteobacteria*, *Patescibacteria* and *Bacteroidota* are negatively correlated with INS and Treg. These bacteria phylum may play a significant role in gut immunity and insulin resistance. But these phyla contain many specific genus and species, with complex interactions between the specific bacteria and immunity. Therefore, more efforts should be paid to the functional role of gut microbiota rather than the identification of specific bacterium species in the further study. Shi *et al*. [55] showed that Tregs were essential for peripheral immune tolerance and preventing autoimmunity and tissue damage. Wen *et al*. [56] reported that the Treg/Th17 ratio was significantly lower in the peripheral blood of IGR and T2DM patients when compared with the normal population, and suggested a Treg/Th17 imbalance may be a risk factor for prediabetes and diabetes patients. Regulatory T cells (Treg) control mitochondrial function and cytokine production by $CD4^+$ effector T cells (Teff) in prediabetes and type 2 diabetes by supporting T helper (Th)17 or Th1 cytokine production, respectively. These data suggest that Treg control of Teff metabolism regulates inflammation differentially in prediabetes compared with type 2 diabetes [48]. Tregs in our study were taken from the intestinal mesenteric lymph nodes. Gut microbiota dysbiosis and changed microbiota metabolites affect the intestinal barrier first and lead to chronic inflammation. Presumably, they have a significant impact on gut barrier function and mucosal immune responses. Therefore, the controversial result may be because the metabolites of gut microbiota first induce local immunity in the gut, and then further affect systemic immunity.

Microbial-related metabolites, such as short-chain fatty acids (SCFAs), Trimetlylamine oxide (TMAO), bile acids, and neurotransmitters are important molecules in the microbiota-host-target organ axis [57]. We observed that cholic acid and muricholic acid were more abundant in the IGR group, but were reversed in the IGR+TZT group. Secondary bile acids antagonize the nuclear membrane farnesoid X receptor (FXR) and the G protein-coupled receptor TGR5 in the intestines. Some bile acid metabolites can both improve as well as exert negative effects on gut barrier tight junction function [51]. Stenman LK *et al*. [58] showed that bile acids and their receptors affect intestinal barrier integrity, and exhibited increased gut permeability in mice fed a diet containing Deoxycholic acid (DCA) compared with mice fed a conventional diet. In addition, DCA exacerbated lipopolysaccharide-induced barrier disruption. Consistent with the findings of Stenman LK *et al*. [58], in our current study, hyocholic acid, cholic acid, 12-ketolithocholic acid, Alpha-muricholic acid, and Deoxycholic acid were significantly elevated in the IGR group, suggesting that these bacterial metabolites may affect the integrity of the intestinal barrier in rats, and leads to the occurrence of metabolic endotoxemia, which in turn causes insulin resistance and accelerates the occurrence of T2DM. In the IGR+TZT group,

hyocholic acid, cholic acid, 12-ketolithocholic acid, Alpha-muricholic acid, and Deoxycholic acid were significantly reduced, indicating that TZT may act on gut microbiota and different bile acids to protect the integrity of the intestinal barrier. Alpha-muricholic acid, cholic acid, and taurine were positively correlated with *Desulfobacterota* in our study. This suggested that TZT may affect the metabolic role or abundance of some bacteria genus or species in phylum *Desulfobacterota* and modulate secondary bile acids.

We used integrative analyses, microbial diversity, and an LC-MS based metabolomics approach to study GM diversity and fecal metabolic variations after TZT administration in IGR rats. Notably, TZT prevented gut dysbiosis in IGR rats by restoring the microbial richness and diversity. Meanwhile, different fecal metabolic profiles were identified after the intervention, and some profiles correlated with altered bacterial levels, suggesting TZT not only altered GM composition but also substantially altered fecal metabolomic profiles related to the gut microbiome, resulting in antidiabetic effects.

5. Conclusions

In this study, Illumina Miseq high-throughput sequencing was used to analyze the distribution characteristics of intestinal flora in four rat groups: ND, ND+TZT, IGR, and IGR+TZT. We sought to identify key bacteria which promoted diabetes to provide further interventions for disease diagnosis and treatment. Our study is the first to explore correlations between the hypoglycemic effects of TZT and T lymphocyte subsets. We showed that TZT changed the gut microbiota composition and significantly reduced $CD4^+$ T numbers in the mesenteric lymph nodes of IGR rats, but its specific interaction mechanisms remain unclear. We used the interaction hypothesis of "Herbal medicine-gut microbiota-metabolites-gut immunity-metabolic disease" to reconstruct a new immune microecological health model and elucidate the clinical significance of immune microecology. Our data provide new ideas for immune microecological regulation and the treatment of metabolic and immune-related diseases. The antidiabetic effects of TZT may also be associated with GM improvement and abundance. We provide new insights on mechanisms underlying the therapeutic benefits of TZT for IGR and T2DM.

Author Contributions

RN and YG designed the research study. BZ performed the research. BZ and RN conducted the study and drafted the manuscript. YG and YJ provided administrative support. BZ and LW collected and assembled data. All authors contributed to editorial changes in the manuscript. All authors read and approved the final manuscript.

Ethics Approval and Consent to Participate

The study was approved by the Ethic Committee of Xinjiang Medical University (IACUC-20201026-24).

Acknowledgment

The authors thank Major Bio-Pharm Technology Co. Ltd., (Shanghai, China) gave support on microbial sequencing. The authors thank Xinjiang Key Laboratory of Molecular Biology for Endemic Disease gave support to the lab research.

Funding

This work was supported by the National Natural Science Foundation of China (no. 81860743); and the Innovation Team Foundation of the Xinjiang Uyghur Autonomous region of China (no. 2022D14009).

Conflict of Interest

The authors declare no conflict of interest.

Supplementary Material

Supplementary material associated with this article can be found, in the online version, at https://doi.org/10.31083/j.fbl2709278.

References

[1] American Diabetes Association. Classification and diagnosis of diabetes: standards of medical care in diabetes-2020. Diabetes Care. 2020; 43: S14–S31.

[2] Li Y, Teng D, Shi X, Qin G, Qin Y, Quan H, *et al*. Prevalence of diabetes recorded in mainland China using 2018 diagnostic criteria from the American Diabetes Association: national cross sectional study. British Medical Journal. 2020; 369: m997.

[3] Eades CE, Leese GP, Evans JMM. Incidence of impaired glucose regulation and progression to type 2 diabetes mellitus in the Tayside region of Scotland. Diabetes Research and Clinical Practice. 2014; 104: e16–e19.

[4] Tian X, Zhang Y, Li H, Li Y, Wang N, Zhang W, *et al*. Palmatine ameliorates high fat diet induced impaired glucose tolerance. Biological Research. 2020; 53: 39.

[5] Paun A, Danska JS. Modulation of type 1 and type 2 diabetes risk by the intestinal microbiome. Pediatric Diabetes. 2016; 17: 469–477.

[6] D'Alessandro G, Antonangeli F, Marrocco F, Porzia A, Lauro C, Santoni A, *et al*. Gut microbiota alterations affect glioma growth and innate immune cells involved in tumor immunosurveillance in mice. European Journal of Immunology. 2020; 50: 705–711.

[7] Allin KH, Tremaroli V, Caesar R, Jensen BAH, Damgaard MTF, Bahl MI, *et al*. Aberrant intestinal microbiota in individuals with prediabetes. Diabetologia. 2018; 61: 810–820.

[8] Nuli R, Cai J, Kadeer A, Zhang Y, Mohemaiti P. Integrative analysis toward different glucose tolerance-related gut microbiota and diet. Frontiers in Endocrinology. 2019; 10: 295.

[9] Uribe-Herranz M, Rafail S, Beghi S, Gil-de-Gómez L, Verginadis I, Bittinger K, *et al*. Gut microbiota modulate dendritic cell antigen presentation and radiotherapy-induced antitumor immune response. Journal of Clinical Investigation. 2020; 130: 466–479.

[10] Spencer SP, Fragiadakis GK, Sonnenburg JL. Pursuing Human-

Relevant Gut Microbiota-Immune Interactions. Immunity. 2019; 51: 225–239.
[11] González Olmo BM, Butler MJ, Barrientos RM. Evolution of the human diet and its impact on gut microbiota, immune responses, and brain health. Nutrients. 2021; 13: 196.
[12] Wang T, Wen Y, Fan X. Myeloid-derived suppressor cells suppress CD4 T cell activity and prevent the development of type 2 diabetes. Acta Biochimica Et Biophysica Sinica. 2018; 50: 362–369.
[13] Luc K, Schramm-Luc A, Guzik TJ, Mikolajczyk TP. Oxidative stress and inflammatory markers in prediabetes and diabetes. Journal of Physiology and Pharmacology. 2019. (in press)
[14] Dong L, Xie J, Wang Y, Zuo D. Gut Microbiota and Immune Responses. Advances in Experimental Medicine and Biology. 2020; 1238: 165–193.
[15] Zheng Y, Ding Q, Wei Y, Gou X, Tian J, Li M, *et al*. Effect of traditional Chinese medicine on gut microbiota in adults with type 2 diabetes: a systematic review and meta-analysis. Phytomedicine. 2021; 88: 153455.
[16] Zheng Y, Gou X, Zhang L, Gao H, Wei Y, Yu X, *et al*. Interactions between gut microbiota, host, and herbal medicines: a review of new insights into the pathogenesis and treatment of type 2 diabetes. Frontiers in Cellular and Infection Microbiology. 2020; 10: 360.
[17] Zhang Y, Gu Y, Ren H, Wang S, Zhong H, Zhao X, *et al*. Gut microbiome-related effects of berberine and probiotics on type 2 diabetes (the PREMOTE study). Nature Communications. 2020; 11: 5015.
[18] Wu TR, Lin CS, Chang CJ, Lin TL, Martel J, Ko YF, *et al*. Gut commensal Parabacteroides goldsteinii plays a predominant role in the anti-obesity effects of polysaccharides isolated from Hirsutella sinensis. Gut. 2019; 68: 248–262.
[19] Xu J, Fu C, Li T, Xia X, Zhang H, Wang X, *et al*. Protective effect of acorn (Quercus liaotungensis Koidz) on streptozotocin-damaged MIN6 cells and type 2 diabetic rats via p38 MAPK/Nrf2/HO-1 pathway. Journal of Ethnopharmacology. 2021; 266: 113444.
[20] Ammon HPT. Boswellic extracts and 11-keto-ß-boswellic acids prevent type 1 and type 2 diabetes mellitus by suppressing the expression of proinflammatory cytokines. Phytomedicine. 2019; 63: 153002.
[21] Lv JN. Clinical study of Uyghur medicine Tangningzi Yabitus tablet in the treatment of diabetes. Chinese Journal of Ethnic Medicine. 2002; 04: 006. (In Chinese)
[22] Chen S, Zhou Y, Chen Y, Gu J. Fastp: an ultra-fast all-in-one FASTQ preprocessor. Bioinformatics. 2018; 34: i884–i890.
[23] Magoc T, Salzberg SL. FLASH: fast length adjustment of short reads to improve genome assemblies. Bioinformatics. 2011; 27: 2957–2963.
[24] Edgar RC. UPARSE: highly accurate OTU sequences from microbial amplicon reads. Nature Methods. 2013; 10: 996–998.
[25] Nuli R, Azhati J, Cai J, Kadeer A, Zhang B, Mohemaiti P. Metagenomics and Faecal Metabolomics Integrative Analysis towards the Impaired Glucose Regulation and Type 2 Diabetes in Uyghur-Related Omics. Journal of Diabetes Research. 2019; 2019: 2893041.
[26] Cole JB, Florez JC. Genetics of diabetes mellitus and diabetes complications. Nature Reviews Nephrology. 2020; 16: 377–390.
[27] Adak A, Khan MR. An insight into gut microbiota and its functionalities. Cellular and Molecular Life Sciences. 2019; 76: 473–493.
[28] Magne F, Gotteland M, Gauthier L, Zazueta A, Pesoa S, Navarrete P, *et al*. The firmicutes/bacteroidetes ratio: a relevant marker of gut dysbiosis in obese patients? Nutrients. 2020; 12: 1474
[29] Wang JH, Kim BS, Han K, Kim H. Ephedra-treated donor-derived gut microbiota transplantation ameliorates high fat diet-induced obesity in rats. International Journal of Environmental Research and Public Health. 2017; 14: 555.
[30] Ahmad A, Yang W, Chen G, Shafiq M, Javed S, Ali Zaidi SS, *et al*. Analysis of gut microbiota of obese individuals with type 2 diabetes and healthy individuals. PLoS ONE. 2019; 14: e0226372.
[31] Wu H, Tremaroli V, Schmidt C, Lundqvist A, Olsson LM, Krämer M, *et al*. The Gut Microbiota in Prediabetes and Diabetes: a Population-Based Cross-Sectional Study. Cell Metabolism. 2020; 32: 379–390.e3.
[32] Lu L, Tang M, Li J, Xie Y, Li Y, Xie J, *et al*. Gut microbiota and serum metabolic signatures of high-fat-induced bone loss in mice. Frontiers in Cellular and Infection Microbiology. 2021; 11: 788576.
[33] Lemos LN, Medeiros JD, Dini-Andreote F, Fernandes GR, Varani AM, Oliveira G, *et al*. Genomic signatures and co-occurrence patterns of the ultra-small Saccharimonadia (phylum CPR/Patescibacteria) suggest a symbiotic lifestyle. Molecular Ecology. 2019; 28: 4259–4271.
[34] Zhang X, Shen D, Fang Z, Jie Z, Qiu X, Zhang C, *et al*. Human gut microbiota changes reveal the progression of glucose intolerance. PLoS ONE. 2013; 8: e71108.
[35] Ran B, Guo CE, Li W, Li W, Wang Q, Qian J, *et al*. Sea buckthorn (Hippophae rhamnoides L.) fermentation liquid protects against alcoholic liver disease linked to regulation of liver metabolome and the abundance of gut microbiota. Journal of the Science of Food and Agriculture. 2021; 101: 2846–2854.
[36] Ruuskanen MO, Åberg F, Männistö V, Havulinna AS, Méric G, Liu Y, *et al*. Links between gut microbiome composition and fatty liver disease in a large population sample. Gut Microbes. 2021; 13: 1–22.
[37] Maya-Lucas O, Murugesan S, Nirmalkar K, Alcaraz LD, Hoyo-Vadillo C, Pizano-Zárate ML, *et al*. The gut microbiome of Mexican children affected by obesity. Anaerobe. 2019; 55: 11–23.
[38] Dekker Nitert M, Mousa A, Barrett HL, Naderpoor N, de Courten B. Altered gut microbiota composition is associated with back pain in overweight and obese individuals. Frontiers in Endocrinology. 2020; 11: 605.
[39] Wei X, Tao J, Xiao S, Jiang S, Shang E, Zhu Z, *et al*. Xiexin Tang improves the symptom of type 2 diabetic rats by modulation of the gut microbiota. Scientific Reports. 2018; 8: 3685.
[40] Gong S, Ye T, Wang M, Wang M, Li Y, Ma L, *et al*. Traditional Chinese medicine formula kang shuai lao pian improves obesity, gut dysbiosis, and fecal metabolic disorders in high-fat diet-fed mice. Frontiers in Pharmacology. 2020; 11: 297.
[41] Li ZR, Jia RB, Luo D, Lin L, Zheng Q, Zhao M. The positive effects and underlying mechanisms of Undaria pinnatifida polysaccharides on type 2 diabetes mellitus in rats. Food and Function. 2021; 12: 11898–11912.
[42] Xie J, Yu R, Qi J, Zhang G, Peng X, Luo J. Pectin and inulin stimulated the mucus formation at a similar level: an omics-based comparative analysis. Journal of Food Science. 2020; 85: 1939–1947.
[43] Li Q, Hu J, Nie Q, Chang X, Fang Q, Xie J, *et al*. Hypoglycemic mechanism of polysaccharide from Cyclocarya paliurus leaves in type 2 diabetic rats by gut microbiota and host metabolism alteration. Science China Life Sciences. 2021; 64: 117–132.
[44] Wastyk HC, Fragiadakis GK, Perelman D, Dahan D, Merrill BD, Yu FB, *et al*. Gut-microbiota-targeted diets modulate human immune status. Cell. 2021; 184: 4137–4153.e14.
[45] Zhou C, Zhou Y, Fang J. Gut Microbiota in Cancer Immune Response and Immunotherapy. Trends in Cancer. 2021; 7: 647–660.
[46] D'Alessandro G, Antonangeli F, Marrocco F, Porzia A, Lauro C,

Santoni A, *et al*. Gut microbiota alterations affect glioma growth and innate immune cells involved in tumor immunosurveillance in mice. European Journal of Immunology. 2020; 50: 705–711.
[47] Brown EM, Kenny DJ, Xavier RJ. Gut Microbiota Regulation of T Cells during Inflammation and Autoimmunity. Annual Review of Immunology. 2019; 37: 599–624.
[48] Liu R, Pugh GH, Tevonian E, Thompson K, Lauffenburger DA, Kern PA, *et al*. Regulatory T Cells Control Effector T Cell Inflammation in Human Prediabetes. Diabetes. 2022; 71: 264–274.
[49] Cipolletta D, Feuerer M, Li A, Kamei N, Lee J, Shoelson SE, *et al*. PPAR-γ is a major driver of the accumulation and phenotype of adipose tissue Treg cells. Nature. 2012; 486: 549–553.
[50] Feuerer M, Herrero L, Cipolletta D, Naaz A, Wong J, Nayer A, *et al*. Lean, but not obese, fat is enriched for a unique population of regulatory T cells that affect metabolic parameters. Nature Medicine. 2009; 15: 930–939.
[51] Ghosh S, Whitley CS, Haribabu B, Jala VR. Regulation of Intestinal Barrier Function by Microbial Metabolites. Cellular and Molecular Gastroenterology and Hepatology. 2021; 11: 1463–1482.
[52] Furusawa Y, Obata Y, Fukuda S, Endo TA, Nakato G, Takahashi D, *et al*. Commensal microbe-derived butyrate induces the differentiation of colonic regulatory T cells. Nature. 2013; 504: 446–450.
[53] Yang W, Cong Y. Gut microbiota-derived metabolites in the regulation of host immune responses and immune-related inflammatory diseases. Cellular & Molecular Immunology. 2021; 18: 866–877.
[54] Han H, Yi B, Zhong R, Wang M, Zhang S, Ma J, *et al*. From gut microbiota to host appetite: gut microbiota-derived metabolites as key regulators. Microbiome. 2021; 9: 162.
[55] Shi H, Chi H. Metabolic control of Treg cell stability, plasticity, and tissue-specific heterogeneity. Frontiers in Immunology. 2019; 10: 2716.
[56] Wen J, Liu Q, Liu M, Wang B, Li M, Wang M, *et al*. Increasing Imbalance of Treg/Th17 Indicates more Severe Glucose Metabolism Dysfunction in Overweight/obese Patients. Archives of Medical Research. 2021; 52: 339–347.
[57] Heianza Y, Sun D, Li X, DiDonato JA, Bray GA, Sacks FM, *et al*. Gut microbiota metabolites, amino acid metabolites and improvements in insulin sensitivity and glucose metabolism: the POUNDS Lost trial. Gut. 2019; 68: 263–270.
[58] Stenman LK, Holma R, Eggert A, Korpela R. A novel mechanism for gut barrier dysfunction by dietary fat: epithelial disruption by hydrophobic bile acids. The American Journal of Physiology-Gastrointestinal and Liver Physiology. 2013; 304: G227–G234.